Kumar, Deepak and Workman, Victoria and O'Brien, Marie Claire and McLaren, Jane S. and White, Lisa J. and Ragunath, Krish and Saiani, Alberto and Gough, Julie and Rose, Felicity R.A.J. (2017) Peptide hydrogels — a tissue engineering strategy for the prevention of oesophageal strictures. Advanced Functional Materials, 27 (38). 1702424/1-1702424/12. ISSN 1616-3028

Peptide Hydrogels—A Tissue Engineering Strategy for the Prevention of Oesophageal Strictures

Deepak Kumar, Victoria L. Workman, Marie O'Brien, Jane McLaren, Lisa White, Krish Ragunath, Felicity Rose, Alberto Saiani, and Julie E. Gough*

Endoscopic treatment of Barrett's oesophagus often leads to further damage of healthy tissue causing fibrotic tissue formation termed as strictures. This study shows that synthetic, self-assembling peptide hydrogels (PeptiGelDesign) support the activity and function of primary oesophageal cells, leading to epithelialization and stratification during in vitro 3D co-culture. Following buffering in culture media, rat oesophageal stromal fibroblasts (rOSFs) are incorporated into a library of peptide hydrogels, whereas mouse oesophageal epithelial cells (mOECs) are seeded on the surface. Optimal hydrogels (PGD-AlphaProC and PGD-CGD2) support mOEC viability (>95%), typical cell morphology (cobblestone-like), and slower migration over a shorter distance compared to a collagen control, at 48 h. Positive expression of typical epithelial markers (ZO-1 and cytokeratins) is detected using immunocytochemistry at day 3 in culture. Furthermore, optimal hydrogels are identified which support rOSF viability (>95%) with homogeneous distribution when incorporated into the hydrogels and also promote the secretion of collagen type I detected using an enzyme linked immunosorbent assay (ELISA), at day 7. A 3D co-culture model using optimal hydrogels for both cell types supports a stratified epithelial layer (expressing involucrin and AE1/AE3 markers). Findings from this study could lead to the use of peptide hydrogels as a minimally invasive endoscopic therapy to manage oesophageal strictures.

1. Introduction

Barrett's oesophagus is a precancerous condition affecting the lower oesophagus. Metaplastic changes occur in the epithelium resulting in the presence of abnormal cells. Specifically, stratified squamous epithelium is replaced by columnar epithelium with the presence of mucous-producing goblet cells. The main contributing factors are thought to be directly related to patients suffering from gastro-oesophageal reflux disease (GORD), where repeated exposure of acid and bile salts from the stomach elicits molecular changes, DNA damage, mutations, and metaplastic changes.[1] Barrett's oesophagus is generally left untreated although the risk of progression to oesophageal cancer is higher than with patients without Barrett's. Oesophageal cancer is reported to be on the rise in the western world, being the eighth most common cancer in the world and the highest cause of cancer amongst Caucasian men (UK and USA).[2] An estimated 52 000 cases (adenocarcinomas) and 398 000 cases (squamous cell carcinoma) occur in 1 year, worldwide.[3]

Current treatment options for early oesophageal cancer includes endoscopic mucosal resection (EMR) and thermal/radio ablation therapy, both of which are generally considered safe, are used widely, are successful in removing abnormal cells and thus decreasing the risk of cancer.[4,5] However, due to additional damage to adjacent healthy tissue, in some cases this elicits inflammatory responses and uncontrolled fibrosis, which could cause subsequent stricture formation (narrowing of the oesophagus). Postoperative stricture incidences are extremely high with a 70–80% risk of occurrence after circumferential EMR.[6,7] Current strategies for stricture therapy involve the use of endoscopic balloon dilation. However, associated complications include perforation, bleeding, and bacteraemia.[8] Alternative intervention is required to help improve current therapies, which would reduce the chances of stricture formation, improve patient outcomes, reduce morbidity, reduce patient revisits, and decrease healthcare systems' costs through reducing repeated dilation therapies and the use of dilators and stents.[5,9]

Emerging, alternative strategies for stricture management and elimination involve tissue engineering therapies through the use of biomaterials. Although a relatively unexplored area,

Dr. D. Kumar, M. O'Brien, Prof. A. Saiani, Prof. J. E. Gough
School of Materials
University of Manchester
Manchester M13 9PL, UK
E-mail: j.gough@manchester.ac.uk

Dr. V. L. Workman, Prof. A. Saiani
Manchester Institute of Biotechnology
University of Manchester
Manchester M13 9PL, UK

Dr. J. McLaren, Dr. L. White, Dr. F. Rose
Centre of Biomolecular Sciences
School of Pharmacy
University of Nottingham
Nottingham NG7 2RD, UK

Prof. K. Ragunath
NIHR Nottingham Digestive Diseases Biomedical Research Unit
Queens Medical Centre Campus
Nottingham University Hospitals NHS Trust
Nottingham NG7 2UH, UK

the leading contributor for the development of biomaterial-based strategies for oesophageal tissue engineering and/or stricture management is the Badylak Laboratory. Decellularized xenograft extracellular matrix (ECM, derived from porcine small intestine submucosa (SIS) and urinary bladder mucosa) scaffolds have been developed in the form of tubular constructs in order to permit complete tissue regeneration.[6,10–12] Pre-clinical studies have demonstrated successful endoscopic surgery to place these tubular constructs over the damaged site in canine models. Observations revealed oesophageal mucosal remodeling with complete re-epithelialization and no stricture formation after 8 weeks.[6,10–12] SIS ECM scaffolds have also been implanted into five human patients. In this clinical study, ECM scaffolds were retained in place using an Ultraflex stent, which was removed between 9 and 18 d after implantation. Results indicated minimal stricture formation and nearly complete mature oesophageal squamous epithelialization by 4 months.[12]

More recent developments have included the use of hydrogels, which have already demonstrated promise for a variety of regenerative medicine and tissue engineering applications. However, they have only recently been explored for gastrointestinal (GI) tract applications, and in particular, the management of oesophageal strictures. Hydrogels have many advantages over decellularized tubular scaffolds, including injectability, use of minimally invasive procedures, capacity for repeat administrations, fine-tuned mechanical properties, ability to fill an irregularly shaped space, and bioactivity to mimic native tissue ECM.[13] For these reasons, decellularized ECM hydrogels have been developed, which may also provide an opportunity for stricture management in the future.

The management of oesophageal strictures using hydrogels is a relatively unexplored area, although a few studies have been performed recently. For example, a steroid-loaded hydrogel (Endolubri jelly) has been sprayed endoscopically into 20 patients as a combined therapy with balloon dilation. Early results are promising where a complete squamous epithelium without stenosis has been witnessed after 3 months.[14,15] Other advancements include the use of Food and Drug Administration (FDA)-approved hydrogels for early treatment and improved prognosis of Barrett's oesophagus with a focus on the lower oesophageal sphincter (LOS; which when weakened can permit GORD to develop in patients). In one study, a range of mucoadhesive hydrogels (Polaxamer 407, cross-linked polyacrylic acid, hydroxypropylmethylcellulose, sodium carboxymethylcellulose, and chitosan) were used as a transport material for the topical delivery of the optical imaging agent hexylaminolevulinate (HAL) into an ex vivo rat model and four, healthy human males. Chitosan was revealed to be the best hydrogel for oesophageal adhesion in vitro and in vivo. Furthermore, in vitro release profiles from chitosan loaded with 40×10^{-3} M of HAL demonstrated that after a residence time of 10 min on the oesophageal wall, the amount of HAL delivered to the epithelium was sufficient to permit fluorescence diagnosis of Barrett's oesophagus. In vivo studies demonstrated that increasing the concentration of chitosan (Protasan) from 1.5% to 1.7% increased adhesivity and the fluorescence signal, with a full thickness layer coating on the mucosa.[16] The remit of

application was entirely focused at improving prognosis. However, a study by Johnson et al.[17] focused on the improvement of the LOS. Here, a nonresorbable polymer (ethylene vinyl alcohol) was injected into the LOS using a sclerotherapy-type needle. During injection, the polymer is a nonviscous liquid, which solidifies rapidly in situ. This medical device (Enteryx) had been made available commercially; however, recent reports of patient injury and death as a result of the device led to the FDA removing it from the market.[17] Alternative types of hydrogel that have recently emerged with promising results are decellularized ECM hydrogels (derived from porcine dermal and urinary bladder matrix (UBM)). After in vivo implantation in a rat abdominal wall defect model, both hydrogels had degraded by 35 d, and UBM hydrogels were found to support greater amounts of myogenesis compared to dermal hydrogels.[13] Decellularized hydrogels are progressing toward clinical trials and are currently being investigated for oesophageal strictures to facilitate repair and reconstruction.

Alternatives to hydrogels made of ECM/biological materials are those made using de novo designed materials. In the past decade, great interest has been shown in the development and use of synthetic, self-assembling peptide hydrogels. A variety of designs of short peptides have been presented that self-assemble into water-swollen networks (hydrogels) above a critical gelation concentration (CGC).[18] Zhang and colleagues devised a family of amphipathic self-assembling peptides based on the alternation of hydrophilic and hydrophobic residues. These peptides are able to self-assemble into β-sheet-rich nanofibrillar structures (fibers of 3 nm and bundles of 10–50 nm[19]) that, above the CGC entangle and/or associate with form hydrogels.[19] The propensity of these peptides to self-assemble and the nature of the nano-structures and overall properties of the hydrogel thus formed are dependent on several factors. These include the amino acid sequence, the starting peptide concentration, and the pH, and type of electrolyte in the medium.[20] Peptide hydrogels are now commercially available from several companies, including Puramatrix (Corning), HydroMatrix (Sigma), Biogelx, and more recently PGD-HydroGels (PeptiGelDesign).

There are several advantages in using synthetic, self-assembling peptide hydrogels including low cost, consistent, controllable manufacturing, the fact that amino acids can be easily metabolized by enzymes in vivo making the gels highly biocompatible,[21] and deliverable endoscopically via spraying or injection.[22] A diverse range of properties are made available through changing both the amino acids present and their order within the peptide sequence. The presence of charged amino acids allows variation in both net charge and charge distribution. Tailored release properties, degradation rates, and mechanical properties are all possible using this system, which is difficult to achieve with natural polymers.[23]

This study proposes the use of self-assembling peptide hydrogels for a novel application to treat and/or manage strictures caused by ER for the removal of metaplastic cells in Barrett's oesophagus. It can be anticipated that after delivery of acellular self-assembling peptide hydrogels to the injured area, cells from healthy adjacent tissue would be able to migrate, produce essential matrix proteins, and permit tissue regeneration. The ability to deliver the hydrogel endosocopically is feasible due to the shear-thinning and self-assembling properties of these

hydrogels.[24] Once the hydrogel is delivered to the injury site, it can be anticipated that host fibroblasts and epithelial cells from adjacent healthy tissue would migrate into the hydrogel, permit re-epithelialization[25] and production of matrix, and permit normal function, which is to act as a protective, semipermeable barrier.[26,27] Rapid restitution of the mucosal barrier would result in a reduced inflammatory response resulting in subsequent modulation of fibrosis.[15] Overall, neo-tissue matrix production and remodeling would occur with the desired native tissue-type matrix composition and mechanical properties.

In order to move toward this ultimate translational goal, initial studies were undertaken in vitro, to understand tissue-specific (stromal fibroblasts and oesophageal epithelial) cell response to a library of synthetic peptide hydrogels. As different cells require unique extracellular matrix conditions,[28] we speculated that each cell type would require a distinct gel property. Uniquely, PeptiGelDesign can provide a family of related peptide hydrogels, each with particular combinations of charge and mechanical properties. Use of the panel allowed us to evaluate oesophageal cell response and characterization of cell function through morphology, viability, migration, and typical marker expression in order to identify optimal hydrogels for each cell type. Furthermore, this study is the first to develop a 3D coculture, composite model using self-assembling peptide hydrogels in order to demonstrate the multilayer and multicellular nature of oesophageal submucosa. Again, the unique properties of this hydrogel system allowed combinations of gels to be layered, providing distinct conditions suitable to support each cell type. This study provides the initial steps to be taken forward for using synthetic peptide hydrogels in oesophageal stricture management and potentially for oesophageal tissue engineering.

2. Results

2.1. Rheological Assessment of Peptide Hydrogels

The stiffness of peptide hydrogels was assessed after buffering in media for 24 h at 37 °C. The initial pH of each hydrogel was different (**Table 1**) and therefore the buffering step in media was critical to allow diffusion of nutrients and molecules into the gels as well as neutralize the pH in order to permit a cell-friendly environment. Statistical analysis revealed that PGD-Alpha1, PGD-Alpha2, PGD-AlphaProC, and PGD-CGD2 hydrogels were significantly stiffer (G') compared to PGD-AlphaProB and PGD-C2 hydrogels ($p < 0.001$; Table 1).

Table 1. Mechanical properties and charge density of peptide hydrogels supplied by PeptiGelDesign.

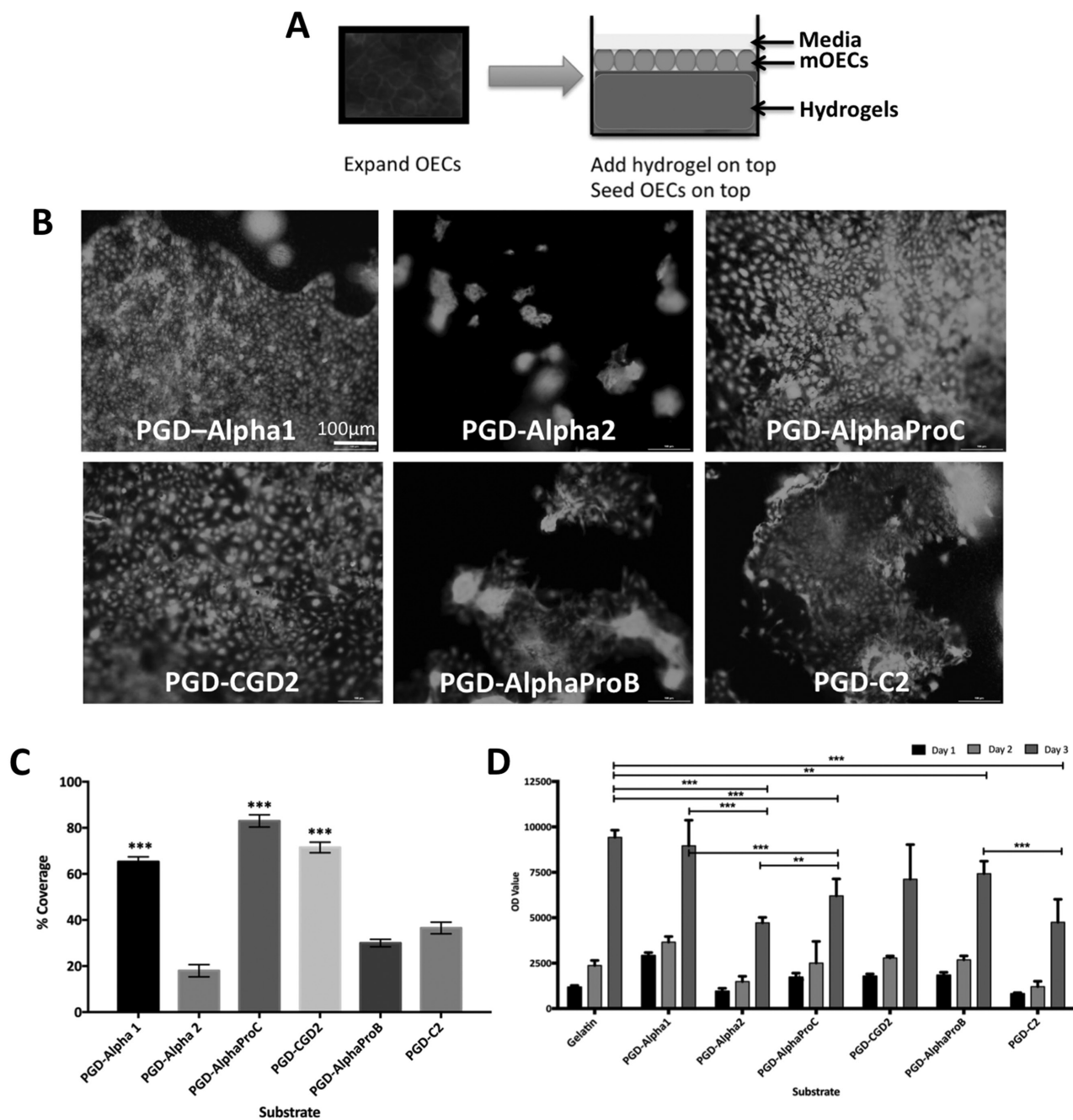| Hydrogel	Stiffness G' after media conditioning for 24 h [Pa]	Initial pH	Charge density
PGD-Alpha1	15 000 ± 5000	3.0–3.5	Neutral
PGD-Alpha2	21 000 ± 1000	4.2–4.8	Low
PGD-AlphaProC	14 000 ± 1300	6.9–7.1	High
PGD-CGD2	5500 ± 1700	6.0–7.0	Low
PGD-AlphaProB	500 ± 80	6.3–6.7	High
PGD-C2	400 ± 10	6.0–6.6	High

2.2. Mouse Oesophageal Epithelial Cell (mOEC) Response to Peptide Hydrogels in 2D Culture

mOECs were cultured on top of peptide hydrogels for 3 d, submerged in media (**Figure 1**A). Viability assessment using the Live/Dead assay revealed that mOECs responded differently depending on which peptide hydrogel surface they were cultured on. However, after 3 d of culture, mOECs appeared viable on all peptide hydrogels as shown in Figure 1B. Obvious effects on mOEC morphology and on ability to form an epithelial sheet were witnessed as a response to the type of peptide hydrogel surface. Observations revealed that PGD-Alpha1, PGD-AlphaProC, and PGD-CGD2 supported typical mOEC morphology and epithelial sheet formation, whereas on PGD-Alpha2, PGD-AlphaProB, and PGD-C2 hydrogels, mOECs appeared to clump together and the epithelial sheet was not as obvious (Figure 1B). Using an ImageJ plug-in Live/Dead, staining images were used to semiquantify epithelial cell coverage. These data further reaffirmed that PGD-Alpha1, PGD-AlphaProC, and PGD-CGD2 supported the greatest epithelial sheet coverage with 81%, 77%, and 65% mOEC coverage on respective peptide hydrogels (Figure 1C). Metabolic activity and proliferation activity of mOECs cultured on top of peptide hydrogels were assessed via the alamarBlue assay. All peptide hydrogels including the control (gelatin-coated tissue culture plastic (TCP), as recommended by manufacturers,;see the "xperimental Section" supported an increase in metabolic activity and proliferation from day 1 to day 3. After 3 d of mOEC culture on top of the peptides, cells cultured on PGD-Alpha1, PGD-CGD2, PGD-AlphaProB, and PGD-C2 displayed similar metabolic activity to the control (gelatin-coated TCP) with insignificant differences (Figure 1D). However, despite supporting similar metabolic activity, hydrogels PGD-Alpha2, PGD-AlphaProB, and PGD-C2 did not support the formation of an intact epithelial cell sheet (Figure 1B).

Optimal peptide hydrogels (PGD-Alpha1, PGD-AlphaProC, and PGD-CGD2) identified from the above data were further investigated to characterize the expression of typical epithelial markers by mOECs. ZO-1 staining in mOECs cultured on optimal peptide hydrogels at day 3 was witnessed, with similar expression to the gelatin control (culture protocol suggested by manufacturer for standard in vitro culture of mOECs), as shown in **Figure 2**. Positive expression of a multipanel of cytokeratins secreted by mOECs was also observed when cultured on optimal peptide hydrogels at day 3. Similar expression patterns were witnessed to the control, as shown in Figure 2, further re-affirming similar mOEC behavior. PGD-AlphaProC and PGD-CGD2 hydrogels were taken forward to a migration assay as these hydrogels supported better expression of ZO-1 and cytokeratins compared to PGD-Alpha1.

2.3. Migration Activity of mOECs Across Peptide Hydrogels During 2D Culture
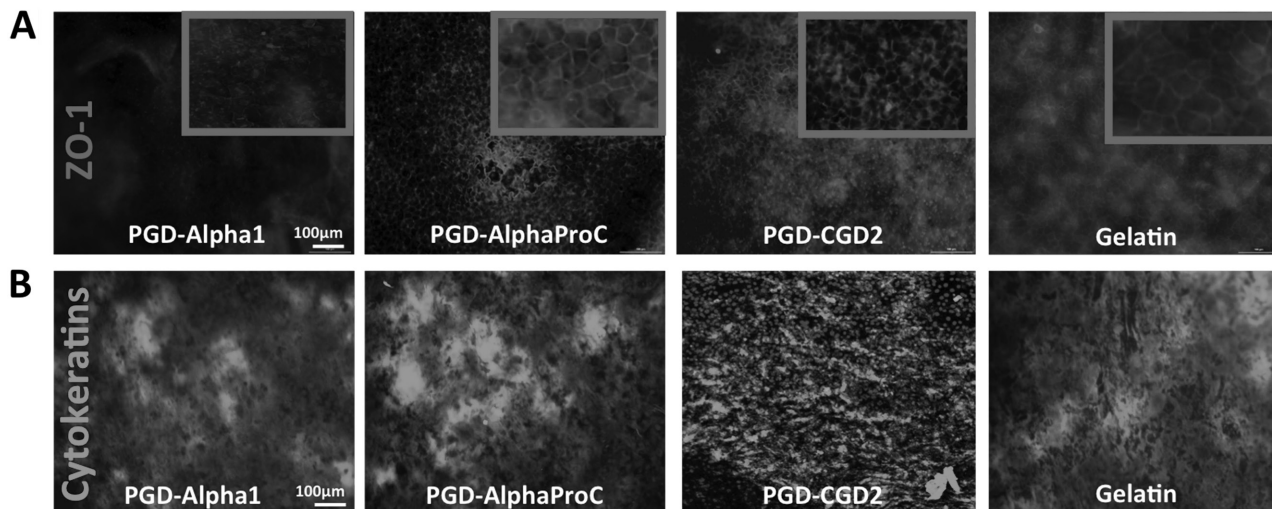
The ability of mOECs to migrate across candidate peptide hydrogels was investigated using a ring migration assay[29] (**Figure 3**A) and time-lapse imaging over a 48 h period. ImageJ was then used to translate pixels into distance covered. Data revealed that migration of mOECs was achieved on both

**ADVANCED
SCIENCE NEWS**
www.advancedsciencenews.com

**ADVANCED
FUNCTIONAL
MATERIALS**
www.afm-journal.de

Figure 1. mOEC behavior when cultured on the surface of peptide hydrogels up to day 3. A) Schematic of experimental setup. B) Viability assessment using Live/Dead assay at day 3. C) Metabolic activity of mOEC assessment using alamarBlue assay up to day 3. D) Epithelial coverage on surface of peptide hydrogels at day 3. Values indicate average viability (D) or average percentage epithelial coverage as determined by image analysis in part (C), ±SD where $n = 3$.

peptide hydrogels (PGD-AlphaProC and PGD-CGD2) and control (collagen hydrogels) over 48 h. mOEC distance covered was significantly greater on collagen hydrogels compared to peptide hydrogels at all time points (20, 24, and 48 h), demonstrated in Figure 3B. However, a significantly greater distance was covered on PGD-AlphaProC (364.4 µm) in comparison to PGD-CGD2 (177.1 µm) at 48 h.

Analysis of migration rate revealed a similar trend to migration distance (Figure 3C). As anticipated, migration rate was significantly faster on collagen hydrogels compared to peptide hydrogels at all time points (20, 24, and 48 h). However, a significantly faster migration rate was witnessed on PGD-AlphaProC (17.432 µm h^{-1}) compared to PGD-CGD2 (10.625 µm h^{-1}) at 48 h. Both hydrogels were seen to support migration of

**ADVANCED
SCIENCE NEWS**

www.advancedsciencenews.com

**ADVANCED
FUNCTIONAL
MATERIALS**

www.afm-journal.de

Figure 2. Characterization of typical epithelial markers. A) ZO-1 marker and B) multipanel of cytokeratins expression by mOECs cultured on the surface of optimal peptide hydrogels at day 3. Scale bar = 100 μm.

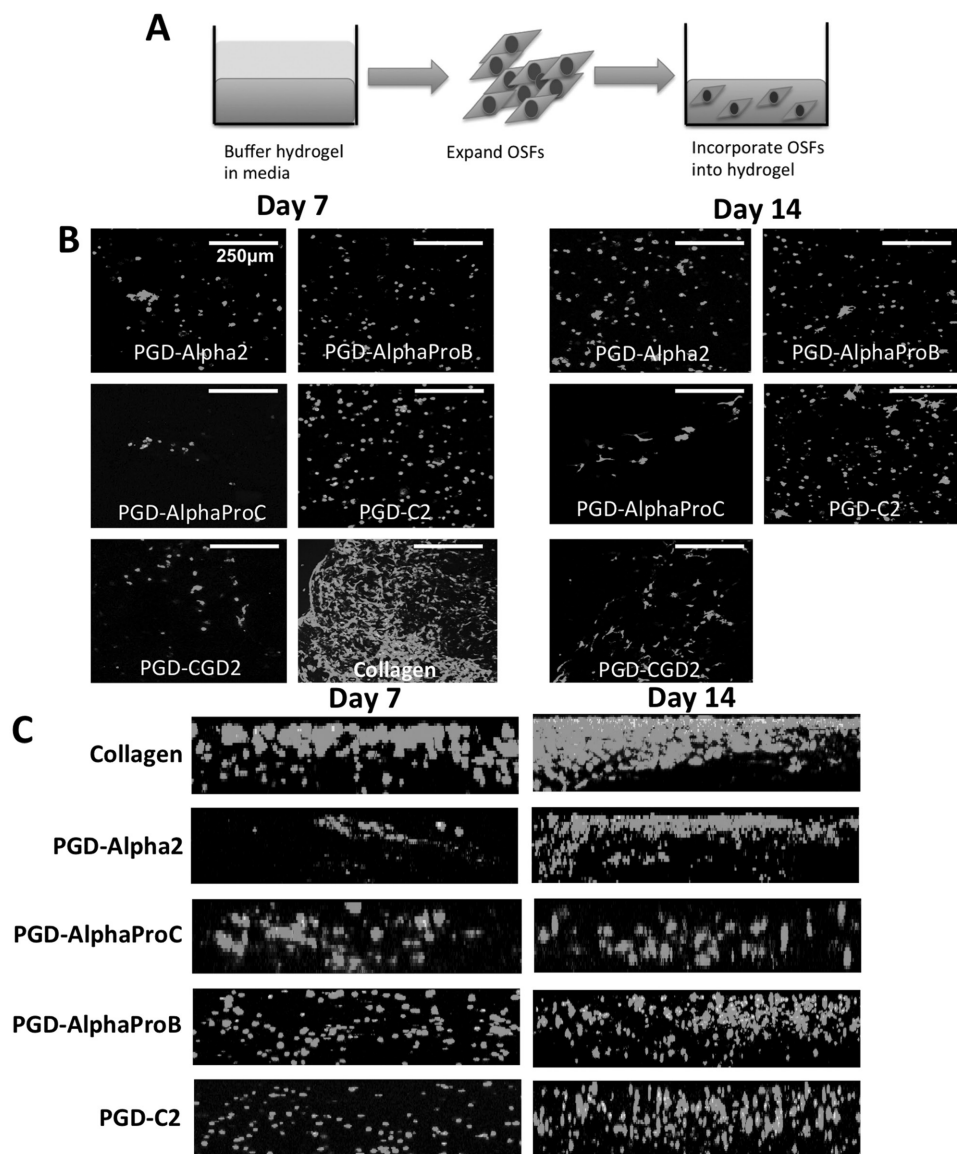epithelial cells and so, taken with the previously presented data, were deemed suitable for culturing mOEC.

2.4. Rat Oesophageal Stromal Fibroblast (rOSF) Response to Peptide Hydrogels in 3D Culture

rOSFs were incorporated into a panel of buffered, peptide hydrogels and cultured up to 7 and 14 d in media, as depicted in

Figure 4A. Live/Dead staining revealed that rOSFs incorporated into all peptide hydrogels remained viable after 7 and 14 d of culture (Figure 4B). Morphological differences in rOSFs were also apparent at day 14, depending on which peptide hydrogels they were cultured in. rOSFs appeared more fibroblastic in PGD-AlphaProC, PGD-C2, and PGD-CGD2 hydrogels, whereas in PGD-Alpha2 and PGD-AlphaProB, rOSFs remained rounded, at day 14. As expected, rOSFs cultured in collagen hydrogels retained their typical fibroblastic-like morphology,
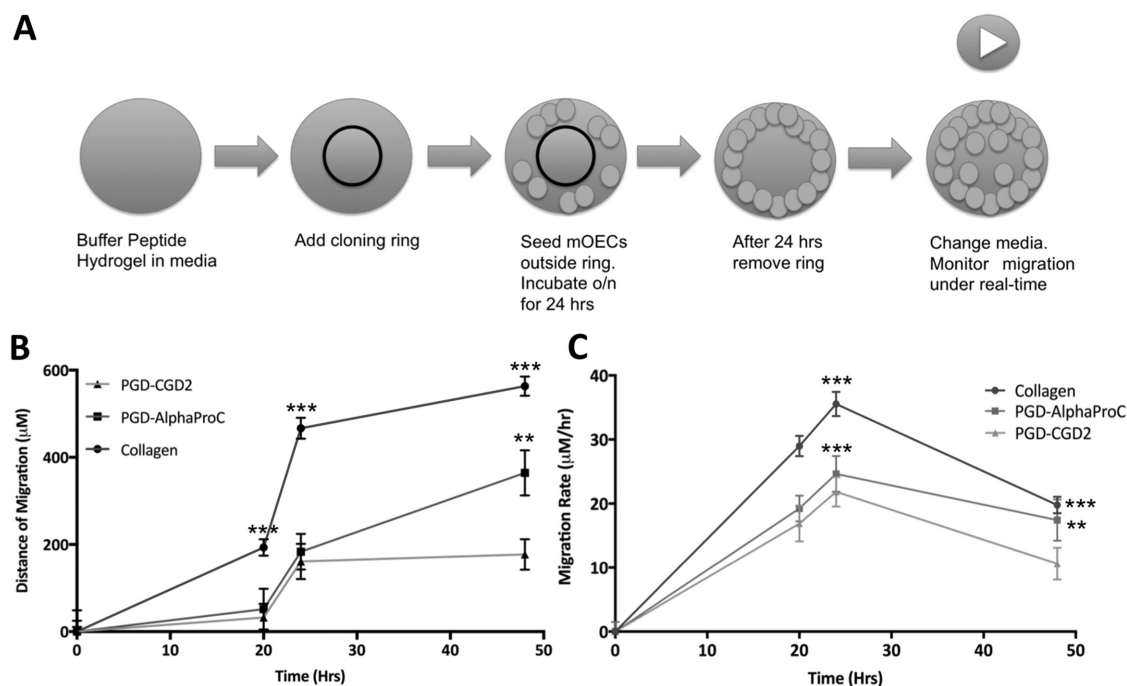
Figure 3. Determination of the migration activity of mOECs across the surface of optimal peptide hydrogels cultured up to 72 h. A) Schematic of experimental setup, B) migration distance, and C) migration rate. Values indicate the average migration distance (μm) or migration rate (μm h^{-1}) and ±SD where $n = 3$.

**ADVANCED
SCIENCE NEWS**
www.advancedsciencenews.com

**ADVANCED
FUNCTIONAL
MATERIALS**
www.afm-journal.de

Figure 4. The behavior of rOSFs embedded within a panel of peptide hydrogels for 3D culture up to day 14. A) Schematic of experimental set-up. B) Assessment of rOSF viability and morphology using Live/Dead assay. C) Assessment of rOSF distribution within the hydrogels using Live/Dead assay. Scale bar = 100 μm.

and more cells were observed to be present on both days 7 and 14 compared to all peptide hydrogels investigated.

Confocal microscopy was used to determine how homogeneously distributed cells were throughout the hydrogel. Studying the distribution of rOSFs in the peptide hydrogels allowed us to establish whether the hydrogel environment supported cell growth and migration, or if cells clustered together in an attempt to survive. Figure 4C represents the full thickness (≈200 μm) view of z-stack Live/Dead images compiled using confocal microscopy. As expected, a greater number of rOSFs were witnessed in collagen hydrogels at days 7 and 14 in comparison to the peptide hydrogels (Figure 4C). rOSFs appeared most homogeneously distributed when encapsulated in PGD-AlphaProB and PGD-C2 (both of which are mechanically weaker gels in the panel, Table 1) at both time points, followed

by collagen hydrogels (Figure 4C). On the contrary, rOSFs appeared to cluster together, and heterogeneously distribute themselves within PGD-Alpha2 and PGD-AlphaProC (both of which are the stiffest gels in the panel, Table 1) at both time points (days 7 and 14).

2.5. Immunohistochemistry and Quantification of Collagen Type I Using ELISA

Type I collagen secretion into the hydrogels by rOSFs was determined via immunohistochemistry. Observations revealed a greater number of rOSFs present in PGD-C2 compared to PGD-AlphaProC at both time points (days 7 and 14). Further to this, greater amounts of type I collagen were present
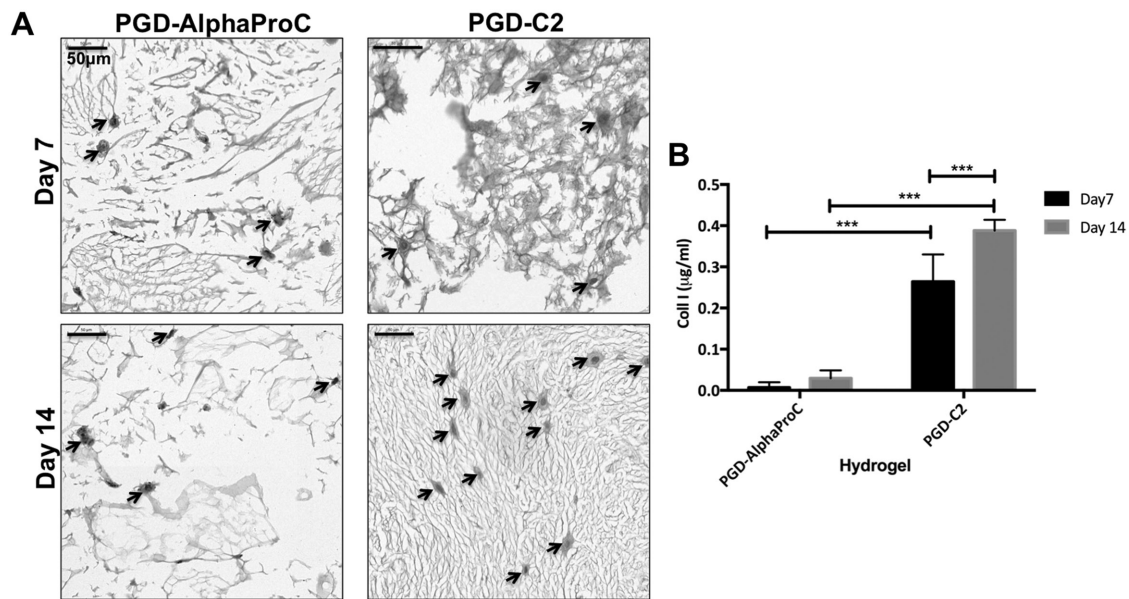
Figure 5. Characterization of type I collagen production. A) Immunohistological images of type I collagen production by rOSFs cultured in PGD-AlphaProC and PGD-C2 hydrogels after 7 and 14 d. B) Quantification of type I collagen production by rOSFs cultured in PGD-AlphaProC and PGD-C2 hydrogels at days 7 and 14. Values indicate mean amount of collagen values ±SD where $n = 3$ (three replicates in a single experiment). Arrows indicate the presence of rOSFs surrounded by deposition of collagen type I within the hydrogels.

surrounding individual rOSFs in PGD-C2 compared to PGD-AlphaProC (**Figure 5**A).

To further determine and quantify the secretion of type I collagen into the hydrogel (PGD-AlphaProC and PGD-C2), collagen was quantified using ELISA in constructs cultured up to days 7 and 14. An increase in collagen production from day 7 to day 14 was witnessed in both hydrogels, PGD-AlphaProC (0.007–0.0295 µg mL^{-1}) and PGD-C2 (0.264–0.3884 µg mL^{-1}). PGD-C2 supported the highest amount of type I collagen production at days 7 and 14 compared to PGD-AlphaProC (Figure 5B).

Taking all the data as a whole, PGD-C2 was seen to be the best peptide hydrogel at supporting rOSF growth, homogeneous distribution and collagen type I secretion. PGD-AlphaProC was also chosen for further investigation, as cells grown in this peptide hydrogel were seen to be more fibroblastic in morphology. We were also interested to determine if a single peptide hydrogel may be suitable for growing both cell types thus simplifying clinical translation; this was an additional reason for selecting PGD-AlphaProC.

2.6. Histological Evaluation of the 3D Co-Culture Composite Model

Optimal performing peptide hydrogels for 2D culture of epithelial cells (PGD-AlphaProC) and 3D culture of fibroblast cells (PGD-C2) were taken forward to produce composite hydrogel systems in order to assess 3D co-culture. Alternative systems were established, namely, system 1 (PGD-AlphaProC for both cell types) and system 2 (PGD-C2 incorporating OSFs; PGD-AlphaProC with OECs on top), and were cultured up to day 7 (**Figure 6**). Histological evaluation using hematoxylin and eosin

(H&E) staining, for both systems, revealed that a successful, uninterrupted layer of mOECs was formed at day 7 with typical multicellular layers. Histological staining for specific epithelial markers revealed that there was positive expression of AE1/AE3 and involucrin for both systems at day 7 (Figure 6). rOSFs were also observed within the bottom hydrogel component of both composite systems, where the rOSFs displayed a rounded morphology.

3. Discussion

This study is the first to report the response of primary oesophageal cells (epithelial cells and stromal fibroblasts) to synthetic self-assembling peptide hydrogels. A library of peptide hydrogels (Table 1) was explored, each displaying unique physical characteristics including stiffness and overall net charge. Due to the complex nature of this study, it was apparent that an available material with easily tailorable mechanical properties (a library) would be beneficial to support each cell type. Self-assembling peptides are infinitely tailorable, and hence were the prime candidate for the remit of this study. The rationale behind using such peptide hydrogels was to identify a synthetic matrix that could support mucosal regeneration as an initial step toward the development of a tissue-engineered therapy for the management of stricture formation following endoscopic treatment for Barrett's oesophagus.

From this study, it was clear that the behavior (morphology, proliferation, and intact epithelial cell sheet formation) of mOECs was influenced by the properties of peptide hydrogels despite demonstrating similar cell viability across the panel. Having a library of various peptide hydrogels allowed the identification of the optimal gel to be chosen for each cell type
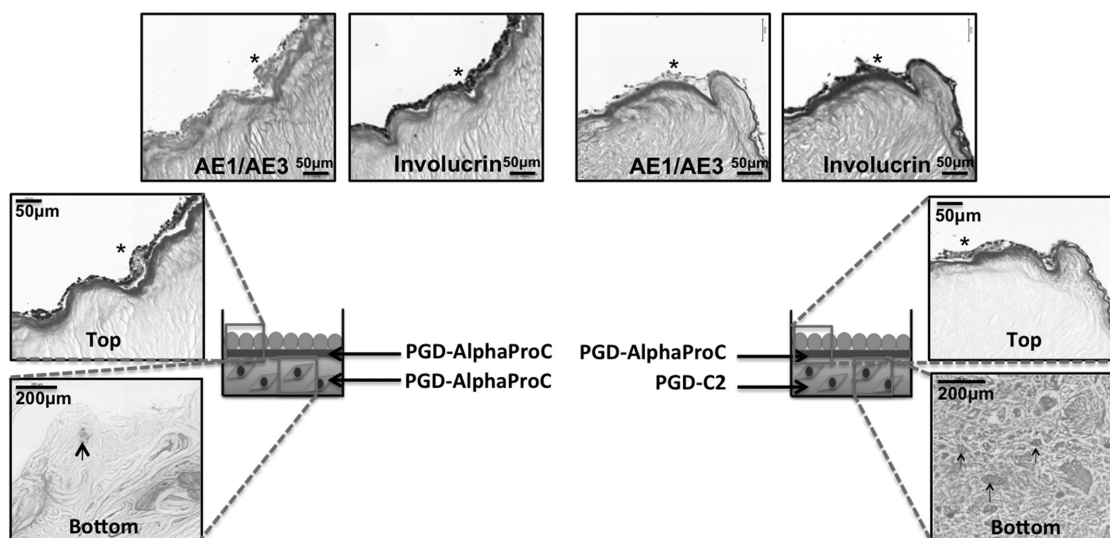
Figure 6. Histological analysis of 3D co-culture composite systems, cultured up to day 14 at air–liquid interface. Schematic of the two co-culture systems (system 1 and system 2) with H&E staining, AE1/AE3 multicytokeratin staining, and involucrin staining. Asterisk indicates the positive expression of specific epithelial markers (AE1/AE3 or involucrin), and the arrows are pointing to single rOSFs with surrounding collagen deposition.

(mOEC and rOSF). Such assays have been performed in studies with a similar remit where the necessity of validating tissue-specific cell behavior and functionality in vitro before moving toward in vivo, were specifically highlighted.[25,27] After 3 d of mOEC culture on top of buffered peptide hydrogels, the preferential peptide hydrogels were identified as PGD-AlphaProC and PGD-CGD2 as demonstrated by the typical cobblestone-like morphology and tight junction formation between cells (ZO-1 expression), resulting in an epithelial sheet-like formation. Positive expression of cytokeratins was also observed. Interestingly, PGD-AlphaProC and PGD-CGD2 were among the stiffest hydrogels in the panel ranging between 5.5 and 14 kPa.

In order to represent the mucosa of the oesophagus (which can be damaged during oesophageal surgery), primary stromal fibroblasts were incorporated and cultured in 3D in buffered peptide hydrogels. Again, differences in behavior in terms of cell morphology and homogeneous distribution were observed and influenced by the properties of the peptide hydrogel. Here, the optimal hydrogels were revealed to be PGD-AlphaProC (the third stiffest in the panel) and PGD-C2 (weakest in the panel at 0.4 kPa) based on the ability of the cells to remain viable and to adopt a fibroblastic phenotype.

The difference in such cell behavior can be attributed to many different material-related aspects. Indeed, each aspect will have a combinatorial effect on cell response; however, for clarity, each aspect will be discussed in turn. The panel of peptides utilized in this study has varying numbers of charged amino acids present, thus varying the charge of the assembled hydrogels. The overall charge carried on hydrogels can heavily influence cell adhesion and behavior. Positively charged surfaces are known to increase cell attachment and proliferation; as demonstrated by Schneider et al.[23] Negatively charged hydrogels have also been shown to increase proliferation of endothelial cells[30] and improve cartilage regeneration in vivo,[31] although Liu et al.[32] observed decreased fibroblast proliferation on negatively charged hydrogels. These differences in findings about

which charge cells favor lead us to speculate that certain cells prefer a specific charge, be it positive or negative. However, our study appears to indicate that the effect of charge is overriding the effect of mechanical properties. The mechanical properties, for example, of PGD-Alpha1 (15 kPa) and PGD-AlphaProC (14 kPa) are very similar, whereas the charges are neutral and highly positive, respectively. Although the mechanical properties are very similar, both cell types responded differently to these two hydrogels. Neither cell type preferred PGD-Alpha1 suggesting that they preferred positively charged material over neutrally charged. There are undoubtedly synergistic responses between mechanical properties, charge, and other factors and charge cannot be said to be the only reason cells prefer the gels they do.

Variations in mechanical properties of the self-assembled hydrogels used in this study can also impact cell response. Differential proliferation rates and cell spreading have been widely reported within hydrogels of different stiffness, as reviewed in Ahearne.[33] Matrix stiffness has also been demonstrated to dictate changes in cell phenotype,[28] cytoskeleton,[34] proliferation,[35] and mobility,[36] as well as drive stem cell differentiation toward specific lineages.[28] Growing both cell types with the panel of hydrogels with different mechanical properties revealed that mOECs appeared to prefer stiffer peptide hydrogels in comparison to rOSFs, which when encapsulated in three dimensions require weak gels for motility. Further analysis revealed that there is a fine line in the preferred stiffness (between 5.5 and 14 kPa) of the hydrogels for mOEC attachment and expansion. On the softer peptides (PGD-AlphaProB and PGD-C2), mOECs were not able to retain a flat epithelial sheet and instead detached away from the hydrogel indicating weak attachment and interaction of mOECs to the surface of these hydrogels. Likewise, on PGD-Alpha2, which was the stiffest hydrogel in the panel, cells could not attach. Further studies would be required to profile cell surface integrin binding and cytoskeleton behavior to elucidate how

**ADVANCED
SCIENCE NEWS**
www.advancedsciencenews.com

**ADVANCED
FUNCTIONAL
MATERIALS**
www.afm-journal.de

well mOECs anchor/interact with the substrate and whether changes in interaction occur as a result in stiffness change.

Hydrogel stiffness also influenced rOSF behavior; in particular, the homogeneous distribution within the hydrogels was enhanced after encapsulation within the softer hydrogels (PGD-AlphaProB and PGD-C2). Interestingly, increase in cell number appeared to remain similar across the panel of hydrogels, as shown visibly in the Live/Dead images from day 7 to day 14, which possibly suggests that the hydrogels may have an inherent property to modulate fibroblastic proliferation activity. However, this property would have to be investigated further. Conclusively, it appears that there is a combination of material-related factors (charge and mechanical properties) that work in synergy to influence the effect on cell response—some of which are yet to be fully defined and understood.

Additional benefits of these peptide hydrogels are that they have a nanofibrillar architectural structure which is similar to that of native ECM, and are shear thinning. This property provides the opportunity to deliver/inject the hydrogel material (either in acellular form or as a cell delivery vehicle) in a minimally invasive manner through endoscopy. This delivery would require minimal deviation from current oesophageal treatments, which take place endoscopically. Furthermore, the peptide hydrogels that mOECs responded well to (PGD-AlphaProC and PGD-CGD2) also possess similar mechanical properties to the native human oesophagus tissue interface (5–50 KPa).[37] In fact, after media conditioning, the majority of the hydrogels on the panel had G' values above 5 kPa, except PGD-AlphaProB and PGD-C2.

As this study was the initial step toward the development of a tissue engineering therapy, future investigations would be required to elucidate the degradation profile of the optimal hydrogels before moving toward in vivo implantation studies. These degradation studies would be needed to confirm that the gel did not degrade/lose mechanical stiffness within the time period required for epithelialization. Through the use of the hydrogel we would anticipate promotion of early epithelialization (in this study epithelial sheet formation was witnessed within 7 d on the hydrogels), which would subsequently minimize associated proinflammatory responses thought to be critical in the prevention of stricture formation.[6] Further in vitro and in vivo studies are required to investigate the ability of the hydrogel to modulate inflammatory responses and fibrotic tissue formation.

As we demonstrated a positive oesophageal cell response to the identified peptide hydrogels in vitro, an alternative strategy to cell-loaded hydrogels could be the delivery of an acellular peptide hydrogel in vivo. Migration data supported the fact that mOECs were able to migrate across the peptide hydrogel surface and permit epithelialization. By replicating this scenario in vivo after implantation, we envisage the migration of epithelial cells from healthy adjacent tissue on to the peptide hydrogel and for the hydrogel to efficiently permit re-epithelialization of the oesophagus. In addition, an acellular product presents a more feasible route to market, and one with less risks and concerns due to the absence of biological material.

This is the first study that has attempted to replicate the in vivo oesophageal mucosa structure (epithelium and stroma, which are usually damaged during endoscopic treatment and surgery) of the oesophagus in vitro by assessing cell response when in 3D co-culture within synthetic peptide hydrogels. Other, in vitro 3D co-culture systems do exist; however, these are developed using xenogenic material.[26,38] For this investigation a composite hydrogel system was formulated as the two different cell types of interest (mOECs and rOSFs) preferentially grew on different hydrogels. The top layer, which supported the epithelial layer, was cultured at air–liquid interface to mimic the in vivo environment of the oesophageal epithelium. Histological analysis of both composite systems (cultured for 7 d) revealed the presence of stromal fibroblasts within the bottom layer hydrogel and a distinct, uninterrupted epithelium layer on the surface of the top-layered hydrogel. On both composites, #1 and #2, the epithelium consisted of 2–3 layers of cells, therefore, indicating epithelium stratification starting to take place after 7 d of culture. The number of cell layers can be attributed to the cross-talk between stromal fibroblasts and epithelial cells when in co-culture. In a similar study, an organotypic model using a mixture of xenogenic material consisting of collagen hydrogel and Matrigel with incorporated stromal fibroblasts was cultured for 7 d before seeding oesophageal epithelial cells on top and continuing culture up to day 15.[26] Despite the contraction of the hydrogel by the stromal fibroblasts, the cross-talk between both cell types promoted a stratified epithelium to be formed on top with the positive expression of involucrin and cytokeratins. In our study the stromal fibroblasts did not visually contract the peptide hydrogels but still supported the formation of an epithelium within an organotypic (co-culture) model.

This study highlighted the difference in fibroblast morphology depending on the culture conditions. For example, a fibroblastic morphology was witnessed when fibroblasts were cultured in 3D whereas under co-culture conditions fibroblasts in fact, remained rounded. It is generally accepted that epithelial cells and fibroblasts in the submucosa communicate via paracrine signals, which influence cell differentiation, function, and proliferation.[27] We hypothesize that this signaling phenomenon may be responsible for the observed differences in morphology of fibroblasts.

It is imperative for the biomaterial of choice to promote stratified epithelialization as this indicates a thick epithelium with appropriate function, such as forming a protective barrier.[39] Only a limited number of studies have attempted to understand epithelial cell interaction to appropriate substrates in vitro; Beckstead et al.[40] investigated oesophageal epithelial behavior on a range of synthetic (polyesters) and natural (Alloderm—decellularized skin graft) scaffolds. Alloderm supported the formation of a 5–6 cell layer epithelium with the expression of loricrin (late stage marker for epithelium; similar to involucrin) after 18 d in culture. On the other hand, the synthetic scaffolds only supported a 2–3 cell layer epithelium which lacked overall spatial organization and formed an interrupted layer. This lack of epithelialization may have been attributed to the pore size, structure, and surface properties of the scaffolds. Synthetically produced peptide hydrogels used in the current study also supported a 2–3 cell layer epithelium, however, in this case, formed a continuous layer within an accelerated time period (7 d) and also expressed late stage differentiation marker (involucrin). The observed outcomes indicate that the structural

**ADVANCED
SCIENCE NEWS**
www.advancedsciencenews.com

**ADVANCED
FUNCTIONAL
MATERIALS**
www.afm-journal.de

and surface properties, as well as the pore size, may be architecturally suitable for supporting the formation of a functional epithelium. Further to this, synthetic peptide hydrogels may eradicate the need to pre-coat synthetic scaffolds with ECM proteins such as collagen and fibronectin to support the expansion of oesophageal epithelial cells, providing a minimally invasive therapy, which is reproducible and could be mass produced.

4. Conclusion

Synthetic peptide hydrogels (PGD-AlphaProC and PGD-CGD2) have been identified to support mOEC adhesion, proliferation, typical morphology, and epithelial cell sheet formation with positive expression of typical markers (AE1/AE3 and involucrin). Additionally, synthetic peptide hydrogels (PGD-AlphaProC and PGD-C2) were identified to support 3D homogeneous distribution of viable rOSFs. A co-culture model was set up containing both cell types (mOECs and rOSFs) demonstrating a multicellular and multilayer hydrogel system. The co-culture system successfully supported the formation of a functional, uninterrupted epithelial sheet within 7 d of culture. This study has highlighted preferential synthetic peptide hydrogels to support cytocompatibility to oesophageal cells and is the initial step in identifying materials suitable or development of a tissue engineering therapy as a postendoscopic treatment for stricture management in Barrett's oesophagus.

5. Experimental Section

Peptide Hydrogels: A library of synthetic, self-assembling peptide hydrogels was purchased from PeptiGelDesign (Cheshire, UK). Each hydrogel is different in terms of peptide sequence, stiffness, and overall charge that the peptide holds. Peptide hydrogels were sterilized by PeptiGelDesign using γ irradiation prior to cell culture. Rheological properties of hydrogel samples were measured after conditioning with media for 24 h at 37 °C in a humidified CO_2 incubator. All rheological studies were undertaken using a stress-controlled rheometer (Discovery HR2, TA Instruments, Herts, UK) equipped with 20 mm parallel plates. In each experiment, 200 µL of sample was loaded onto the stage and the upper plate lowered until a 500 µm gap was reached. All readings were taken at 37 °C. At least once for each sample, amplitude sweeps were performed at a fixed frequency of 1 Hz in the 0.1–10% strain range to determine the linear viscoelastic region (LVR) of each sample. Frequency sweeps were then performed at 1% strain, within the LVR of the samples. Thereafter, measurements of G' and G'' were recorded at 0.2% strain and frequency of 1 Hz. All measurements were repeated at least three times to ensure reproducibility.

Oesophageal Cell Expansion: Primary mouse oesophageal epithelial cells were purchased from CellBiologics (catalog #: C57-6046, USA) and cultured as instructed per manufacturers' protocol. Briefly, flasks were pre-coated with 0.2% gelatin (30 min at room temperature (RT)), washed twice with phosphate buffered saline (PBS), and seeded with OECs. Cells were cultured in epithelial cell medium and supplement kit (catalog #M6621-kit; Caltag, UK), which consisted of basal media supplemented with 2×10^{-3} M L-glutamine (LG), antibiotic antimycotic solution (A&A ; 100 U penicillin, 0.1 µg streptomycin, and 0.25 µg mL^{-1} amphotericin), 5% fetal bovine serum (FBS), insulin–transferrin–sodium selenite, hydrocortisone, and epidermal growth factor. Media changes took place every other day, and cells were passaged at ≈70% confluence using trypsin (0.5 g; Sigma, T3924) and reseeded at a split ratio of 1:3.

Primary rat oesophageal stromal fibroblasts were directly isolated from Sprague Dawley rat oesophageal stromal tissue donated as waste

tissue from a different animal study. After sacrifice, oesophagus tissue was washed in PBS with A&A (100 U penicillin, 0.1 µg streptomycin, and 0.25 µg mL^{-1} amphotericin) for 5 min, followed by two PBS washes. Tissue was treated with dispase I (4 U mL^{-1}; Sigma, Dorset, UK) overnight at 4 °C. The following day, oesophagus tissue was cut longitudinally and the epithelial layer removed. The remaining stromal tissue was cut, diced into small pieces, and treated with sterile filtered collagenase type II dissolved in Hanks solution (100 U mL^{-1}; Gibco, UK) for 2 h in a water bath at 37 °C. Brief vortexing took place every 20 min. Tissue in collagenase II solution was quenched in media consisting of Dulbecco's modified Eagle's medium (DMEM) high-glucose supplemented with 10% FBS, 2×10^{-3} M LG, and A&A (100 U penicillin, 0.1 µg streptomycin, and 0.25 µg mL^{-1} amphotericin), and then passed through a cell strainer (70 µm pore size). Cell solution was centrifuged at 1400 rpm for 3 min, supernatant removed and the fibroblasts (1×10^6 cells) plated out per T75 flask with the same media used for quenching. Cells were incubated at 37 °C, and a media change took place after 48 h and approximately every 2 d as necessary thereafter.

Oesophageal Cell Culture with Peptide Hydrogels: Peptide hydrogels were pipetted into 24-well ThinCerts (Griener, UK) and pre-equilibrated in media, overnight, to pH 7. Media were removed, and cells were introduced using the following protocols.

Oesophageal Cell Culture with Peptide Hydrogels—2D Culture of OECs: OECs were trypsinized and a cell suspension was prepared at a density of 3000 cells mm^{-2}/20 µL. Cell suspension was seeded directly on top of hydrogels (100 µL volume) and incubated for 30 min before submerging with media by adding to the surrounding areas of the insert in the well. Cell–gel constructs were expanded up to day 3 with media changes taking place every day. Controls used were gelatin-coated-glass coverslips.

Oesophageal Cell Culture with Peptide Hydrogels—3D Culture of OSFs: OSFs were trypsinized, and a cell suspension was prepared at a density of 200 000 cells/10 µL. Media were removed from buffered hydrogels, and cell suspension was injected using a 10 µL pipette tip into the hydrogel (150 µL) to give a final seeding density of 200 000 cells/150 µL volume of hydrogel. The cells were homogeneously integrated by mixing the cell suspension with the hydrogel using a pipette tip. OSF-laden hydrogels were incubated for 15 min to allow reassembly of the hydrogel network and then immersed in media. Media changes took place every 3–4 d and cell–gel constructs were cultured up to days 7 and 14. Controls used were collagen hydrogels (Rat tail, type I collagen; Millipore, UK).

Oesophageal Cell Culture with Peptide Hydrogels—3D Co-Culture: The optimal performing peptide hydrogels for 2D culture (PGD-AlphaProC) and 3D culture (PGD-C2) were taken forward for this experiment. Two systems were investigated: system 1 (PGD-AlphaProC for both cell types) and system 2 (PGD-C2 incorporated with OSFs and PGD-AlphaProC with OECs on top). OSFs (500 000 cells/10 µL) were incorporated into buffered PGD-AlphaProC or PGD-C2 peptide hydrogels, using the procedure stated previously. After 5 d of culture, 50 µL of PGD-AlphaProC was added on top of PGD-AlphaProC (system 1) and PGD-C2 (system 2). Stromal fibroblast media were added on top to buffer the peptide hydrogels for 2 h in the incubator at 37 °C. Media were removed, and OECs (3000 cells mm^{-2}/20 µL) were seeded on top of the hydrogels and incubated for 2 h to allow attachment. Stromal fibroblast media were removed from the top and fresh stromal fibroblast media were added around the inserts, allowing the top layer to be cultured at the air–liquid interface. Composites were cultured at 37 °C until days 7 and 14, with media changes taking place every 3–4 d.

OEC Viability Analysis on Peptide Hydrogels: Cell viability with hydrogels was investigated using a Live/Dead cell double staining kit (Sigma, Dorset, UK). Media were removed from cell–hydrogel samples and controls, washed twice with PBS and stained with calcein-AM and propidium iodide solution as per manufacturer's instructions. Briefly, samples were immersed in staining solution and incubated at 37 °C for 15–20 min. Staining solution was removed from samples, washed twice with PBS and imaged with a confocal microscope using 490 nm/515 nm (excitation/emission) for calcein-AM and 535 nm/617 nm (excitation/emission) for

propidium iodide. Semiquantification of epithelial coverage on peptide surfaces was calculated using an ImageJ plug-in where Live/Dead staining images were used. Briefly, the threshold was adjusted to detect the difference between green and black, and then analyzed to quantify percentage coverage.

OEC Metabolic and Proliferation Activity on Peptide Hydrogels: Metabolic activity of OECs was evaluated using the alamarBlue assay (5×10^{-3} M, prepared in PBS; Sigma, Aldrich, UK). Media were removed from samples, washed twice in PBS (immersed in PBS for 5 min each time), and then incubated in alamarBlue solution at 37 °C for 2 h. Absorbance values were taken after 2 h in culture at 570 nm/585 nm (excitation/emission) using a BMG LABTECH plate reader. alamarBlue solution was removed, and samples were thoroughly washed in PBS and cultured in fresh media until the next time point.

Migration Assay: 12 well ThinCerts were coated with 200 µL of hydrogel (PGD-AlphaProC, PGD-CGD2 and collagen) and buffered in media overnight, inside a 12-well plate. A snipped pipette tip was used to act as a cloning ring and a barrier to cell seeding and placed centrally on top of the hydrogel. OECs were trypsinized, and a cell seeding solution of 60 000 cells/50 µL was prepared. Cell solution was seeded on top of the hydrogel around the outer perimeter of the barrier. Constructs were carefully incubated at 37 °C for 1 h to allow cell attachment to hydrogel. Media were added around the insert and samples then incubated overnight. On the following day, the barrier was removed, media changed and samples transferred to the JuLi Br & FL station microscope (NanoEnTek) in the incubator. Cell migration over 72 h was monitored using time-lapse imaging. Cell migration rate and distance was calculated using ImageJ.[41]

Characterization of Marker Expression of OECs Cultured on Peptide Hydrogels: Media were removed from OECs cultured on top of hydrogels for 3 d. Hydrogels were washed with PBS and fixed in 10% formalin solution (neutral buffered; HT5012, Sigma-Aldrich, UK) at RT for 10–15 min. Fixative was removed and hydrogels treated with permeabilization/blocking buffer (0.1% Triton X-100, 1% bovine serum albumin (BSA), and 1% goat serum, in PBS) for 30 min at RT. Marker expression was assessed using the following methods:

Characterization of Marker Expression of OECs Cultured on Peptide Hydrogels—ZO-1: Hydrogels were treated with 2.5 µg mL^{-1} primary ZO-1 antibody (rabbit ZO-1 anti-mouse; 61–7300, Invitrogen, UK,) diluted in the same blocking buffer for 2 h at RT. Hydrogels were washed twice with PBS and treated with a goat anti-rabbit Alexa Fluor 546 secondary antibody (5 µg mL^{-1}, catalog #: A11010; Invitrogen, UK) for 45 min at RT. After treatment, hydrogels were washed twice in PBS and counterstained with 4′,6-diamidino-2-phenylindole (DAPI) for 10 min at RT. Samples were imaged using fluorescence microscopy (Nikon Eclipse 50i Microscope).

Characterization of Marker Expression of OECs Cultured on Peptide Hydrogels—Cytokeratin: Hydrogels were treated with mouse monoclonal anti-pan cytokeratins conjugated with fluorescein isothiocyanate (FITC) (1:50, catalog #: F3418, Sigma, UK) at 4 °C overnight. On the following day, samples were washed twice with PBS and counterstained with DAPI for 10 min at RT and imaged using fluorescence microscopy (Nikon Eclipse 50i Microscope).

Histological Staining of 3D Co-Cultures: Composites cultured for 7 and 14 d were fixed in 10% formalin for 1 h and washed twice with PBS. Composites were then processed overnight using a VIP 2000 (Vacuum Infiltration Processor, Miles Scientific). Samples were embedded in Paraplast paraffin wax (Sigma) and sectioned transversely using a Leica RM2145 microtome. Samples were sectioned at 5 µm and attached to Poly-L-lysine slides (Thermo Scientific).

Histological Staining of 3D Co-Cultures—H&E Staining: Sections were de-waxed in xylene for 5 min, followed by re-hydration in descending grades of ethanol to water. They were stained with hematoxylin for 5 min and "blued" in running water for 5 min. Sections were stained in Eosin Y for 2 min followed by three 1 min washes in 95% ethanol. Sections were then washed in absolute ethanol ×3 and "cleared" in xylene. Sections were then mounted with DPX mount (Sigma). Samples were imaged using a LEICA DMRB fluorescence microscope.

Histological Staining of 3D Co-Cultures—Involucrin and Collagen Type I Immunohistochemical Staining: Sections were de-waxed in xylene for 5 min, followed by rinsing in descending grades of ethanol. They were then placed into methanol/H$_2$O$_2$ to block any endogenous peroxidase (30 min at RT) and finally rinsed in distilled water for 5 min. Antigen retrieval was performed using citrate pH 6 buffer (incubating at 96 °C, for 30 min). Sections were then blocked using R.T.U horse serum (10 min at RT). Primary antibody treatment (rabbit involucrin anti-mouse: 1:1000, overnight at 4 °C; catalog #: Biolegend-924401; Biolegend, USA) or (rabbit Collagen I anti-rat: 1:500, overnight at 4 °C; catalog #: ab34710; Abcam, UK) was followed by secondary antibody treatment with R.T.U ImmPRESS anti-rabbit immunoglobulin G (IgG) (catalog #: Vector-MP-7401) for 30 min at RT. Sections were then treated with 3,3′-diaminobenzidine (DAB) substrate (Vector) for 5 min and counterstained with Nuclear Fast Red (Vector) for 2 min. Sections were then de-hydrated to xylene and coverslips mounted with DPX mountant (Sigma). Samples were imaged using fluorescence microscopy (Nikon Eclipse 50i Microscope).

Histological Staining of 3D Co-Cultures—AE1/AE3 Immunohistochemistry Staining: Sections were de-waxed in xylene for 5 min, followed by rinsing in descending grades of ethanol. Sections were then placed into methanol/H$_2$O$_2$ to block any endogenous peroxidase (30 min at RT) and then washed in distilled water for 5 min. Antigen retrieval was performed using proteinase K (37 °C, for 10 min). Sections were then blocked in 2.5% goat serum (10 min at RT) followed by staining with primary antibody (mouse-IgG1 AE1/AE3 anti-rat, 1:20 dilution, overnight at 4 °C; catalog #: Thermo-MA1-82041; ThermoFisher, UK). After removal of primary antibody, sections were treated with secondary antibody (1:200, biotinylated goat anti-mouse IgG, 30 min at RT). Sections were then treated with avidin–biotin complex (Vector, UK) for 30 min at RT, washed in PBS for 5 min and then treated with DAB substrate (Vector, UK) for 5 min. Sections were counterstained with Nuclear Fast Red (Vector, UK) for 2 min, dehydrated to xylene and cover-slipped using DPX mountant (Sigma). Samples were imaged using fluorescence microscopy (Nikon Eclipse 50i Microscope).

Quantification of Collagen Type I enzyme linked immunosorbent assay (ELISA): Media were removed from hydrogels (PGD-AlphaProC and PGD-C2) incorporated with rOSFs and cultured for 7 and 14 d. Samples were washed with PBS and stored at −80 °C. Solubilization of collagen was achieved by breaking up the cell–gel constructs using acetic acid (0.05 M acetic acid) and transferring to a microcentrifuge tube, to which pepsin solution was added (0.1 mg mL^{-1}). Collagen digestion took place at 4 °C for 24 h with gentle mixing on a rotor with occasional vigorous mixing by hand. Samples were then centrifuged (10 000 rpm, 3 min) and supernatants collected and transferred into collection tubes. Supernatants were stored and analyzed to detect collagen type I as per manufacturers' instructions using ELISA (product code: 6013, Rat, Chondrex, USA). Optical densities (ODs) of ELISA samples were read at 490 nm using the BMG LABTECH plate reader.

Statistical Analysis: Means and standard deviations (SDs) were calculated from three repeats on each sample, except for alamarBlue quantification data, where triplicate readings were performed for each repeat. Error bars on graphs represent SD in both positive and negative orientation. Data were tested for normality and a one-way (Figure 2C) or two-way (Table 1, Figures 2D, 4B,C) analysis of variance (ANOVA)/ Kruskall–Wallis test was performed, followed by a Tukey's posthoc test to determine the significance of origin for all data. Significance levels were defined as: *$p < 0.05$, **$p < 0.01$, and ***$p < 0.001$.

Acknowledgements

Conflict of Interest

The authors declare no conflict of interest.

Keywords

[1] R. C. Fitzgerald, *Gut* **2006**, *55*, 1810.
[2] C. P. Wild, L. J. Hardie, *Nat. Rev. Cancer* **2003**, *3*, 676.
[3] R. Londono, S. Badylak, *Tissue Eng., Part B* **2015**, *21*, 393.
[4] J. Mannath, K. Ragunath, *Ther. Adv. Gastroenterol.* **2010**, *4*, 275.
[5] P. M. Shah, H. Gerdes, *J. Gastrointest. Oncol.* **2015**, *6*, 20.
[6] A. Nieponice, K. McGrath, I. Qureshi, E. J. Beckman, J. D. Luketich, T. W. Gilbert, S. F. Badylak, *Gastrointest. Endosc.* **2009**, *69*, 289.
[7] B. Qumseya, W. David, M. McCrum, Y. Dong, M. Raimondo, T. A. Woodward, M. B. Wallace, H. C. Wolfsen, *Am. J. Gastroenterol.* **2014**, *109*, 369.
[8] K. Uno, K. Iijima, T. Koike, T. Shimosegawa, *World J. Gastroenterl.* **2015**, *21*, 7120.
[9] P. D. Siersema, *Nat. Clin. Pract. Gastroenterol. Hepatol.* **2008**, *5*, 142.
[10] S. Badylak, D. A. Vorp, A. R. Spievack, A. Simmons-Byrd, J. Hanke, D. O. Freytes, A. Thapa, T. W. Gilbert, A. Nieponice, *J. Surg. Res.* **2005**, *128*, 87.
[11] S. Badylak, S. Meurling, M. Chen, A. Spievack, A. Simmons-Byrd, *J. Pediatr. Surg.* **2000**, *35*, 1097.
[12] S. F. Badylak, T. Hoppo, A. Nieponice, T. W. Gilbert, J. M. Davison, B. A. Jobe, *Tissue Eng., Part A* **2011**, *17*, 1643.
[13] M. T. Wolf, K. A. Daly, E. P. Brennan-Pierce, S. A. Johnson, C. Carruthers, A. D'Amore, S. P. Nagarkar, S. S. Velankar, S. F. Badylak, *Biomaterials* **2012**, *33*, 7028.
[14] H. Mori, H. Kobara, K. Rafiq, N. Nishiyama, S. Fujhara, M. Ayagi, T. Yachida, K. Kato, T. Masaki, *World J. Gastroenterol.* **2013**, *19*, 5195.
[15] F. Yang, D. Ma, Q. Cai, Z. Li, *J. Gastroenterol. Hepatol.* **2013**, *28*, 1795.
[16] S. Collaud, T. Warloe, O. Jordan, R. Gurny, N. Lange, *J. Controlled Release* **2007**, *123*, 203.
[17] D. A. Johnson, R. Ganz, J. Aisenberg, L. B. Cohen, J. Deviere, R. Foley, G. B. Haber, J. H. Peters, G. A. Lehman, *Am. J. Gastroenterol.* **2003**, *98*, 1921.
[18] S. R. Caliari, J. A. Burdick, *Nat. Methods* **2016**, *13*, 405.
[19] S. G. Zhang, D. M. Marini, W. Hwang, S. Santoso, *Curr. Opin. Chem. Biol.* **2002**, *6*, 865.
[20] Y. Hong, R. L. Legge, S. Zhang, P. Chen, *Biomacromolecules* **2003**, *4*, 1433.
[21] A. Markey, V. L. Workman, I. A. Bruce, T. J. Woolford, B. Derby, A. F. Miller, S. H. Cartmell, A. Saiani, *J. Pept. Sci.* **2016**, *23*, 148.
[22] L. A. Castillo Diaz, A. Saiani, J. E. Gough, A. F. Miller, *J. Tissue Eng.* **2014**, *5*.
[23] G. B. Schneider, A. English, M. Abraham, R. Zaharias, C. Stanford, J. Keller, *Biomaterials* **2004**, *25*, 3023.
[24] S. Wan, S. Borland, S. M. Richardson, C. L. Merry, A. Saiani, J. E. Gough, *Acta Biomater.* **2016**, *46*, 29.
[25] A. Saxena, H. Ainoedhofer, M. E. Hollwarth, *J. Pediatr. Surg.* **2009**, *44*, 896.
[26] J. Kalabis, G. S. Wong, M. E. Vega, M. Natsuizaka, E. S. Robertson, M. Herlyn, H. Nakagawa, A. K. Rustgi, *Nat. Protoc.* **2012**, *7*, 235.
[27] Y. Zhu, M. F. Leong, W. F. Ong, M. B. Chan-Park, K. S. Chian, *Biomaterials* **2007**, *28*, 861.
[28] A. J. Engler, S. Sen, H. L. Sweeney, D. E. Discher, *Cell* **2006**, *126*, 677.
[29] A. M. Das, A. M. M. Eggermont, T. L. M. ten Hagen, *Nat. Protoc.* **2015**, *10*, 904.
[30] Y. M. Chen, R. Ogawa, A. Kakugo, Y. Osada, J. P. Gong, *Soft Matter* **2009**, *5*, 1804.
[31] K. Yasuda, N. Kitamura, J. P. Gong, K. Arakaki, H. J. Kwon, S. Onodera, Y. M. Chen, T. Kurokawa, F. Kanaya, Y. Ohmiya, Y. Osada, *Macromol. Biosci.* **2009**, *9*, 307.
[32] D. Liu, T. Wang, X. Liu, Z. Tong, *Biopolymers* **2014**, *101*, 58.
[33] M. Ahearne, *Interface Focus* **2014**, *4*, 1.
[34] S. R. Peyton, A. J. Putnam, *J. Cell. Physiol.* **2005**, *204*, 198.
[35] K. Bott, Z. Upton, K. Schrobback, M. Ehrbar, J. A. Hubbell, M. P. Lutolf, S. C. Rizzi, *Biomaterials* **2010**, *31*, 8454.
[36] C. M. Lo, H. B. Wang, M. Dembo, Y. L. Wang, *Biophys. J.* **2000**, *79*, 144.
[37] J. B. Frokjaer, S. D. Anderson, S. Lundbye-Christensen, P. Funch-Jensen, A. M. Drewes, H. Gregersen, *Neurogastroenterol. Motil.* **2006**, *18*, 104.
[38] N. H. Green, B. M. Corfe, J. P. Bury, S. MacNeil, *J. Visualized Exp.* **2015**, *99*.
[39] R. C. Orlando, *Best Pract. Res., Clin. Gastroenterol.* **2010**, *24*, 873.
[40] B. L. Beckstead, S. Pan, A. D. Bhrany, A. M. Bratt-Leal, B. D. Ratner, C. M. Giachelli, *Biomaterials* **2005**, *6217*, 26.
[41] W. S. Rasband, *ImageJ*, U. S. National Institutes of Health, Bethesda, MD, USA **1997**, http://imagej.nih.gov/ij/.